

UC Berkeley

UC Berkeley Previously Published Works

Title

Hierarchical Silicon Nanospikes Membrane for Rapid and High-Throughput Mechanical Cell Lysis

Permalink

<https://escholarship.org/uc/item/4zm5f5mp>

Journal

ACS Applied Materials & Interfaces, 6(10)

ISSN

1944-8244

Authors

So, Hongyun
Lee, Kunwoo
Seo, Young Ho
et al.

Publication Date

2014-05-28

DOI

10.1021/am501221b

Peer reviewed

Hierarchical Silicon Nanospikes Membrane for Rapid and High-Throughput Mechanical Cell Lysis

Hongyun So,^{†,*} Kunwoo Lee,[‡] Young Ho Seo,[§] Niren Murthy,[‡] and Albert P. Pisano[†]

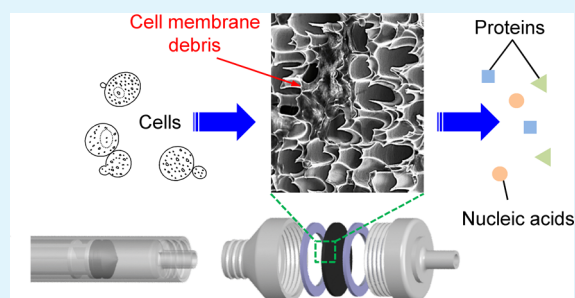
[†]Department of Mechanical Engineering, Berkeley Sensor & Actuator Center and [‡]Department of Bioengineering, University of California, Berkeley, California 94720, United States

[§]Department of Mechanical and Mechatronics Engineering, Kangwon National University, Chuncheon, Gangwon-do 200-701, South Korea

S Supporting Information

ABSTRACT: This letter reports an efficient and compatible silicon membrane combining the physical properties of nanospikes and microchannel arrays for mechanical cell lysis. This hierarchical silicon nanospikes membrane was created to mechanically disrupt cells for a rapid process with high throughput, and it can be assembled with commercial syringe filter holders. The membrane was fabricated by photoelectrochemical overetching to form ultrasharp nanospikes in situ along the edges of the microchannel arrays. The intracellular protein and nucleic acid concentrations obtained using the proposed membrane within a short period of time were quantitatively higher than those obtained by routine, conventional acoustic and chemical lysis methods.

KEYWORDS: hierarchical structure, porous silicon membrane, ultrasharp nanospikes, electrochemical etching, cell lysis, point-of-care diagnostics



Cell lysis is a basic and core technique for the extraction of intracellular proteins and nucleic acids in most biochemical and biophysics research fields. The advent of lab-on-a-chip (LOC) significantly impacted on the development of new lysis tools, which are compact and compatible with microfluidic devices, to improve the efficiency of routine processes for sample preparation.^{1–3} Many conventional cell lysis approaches including chemical,⁴ electrical,^{5–7} thermal,⁸ optical,^{9,10} and acoustic^{11,12} methods need multiple steps that affect the integrity of extracted proteins and nucleic acids. Those methods also require specialized equipment such as electrical sources, a centrifuge, heater, laser or sonicator which might limit point-of-care diagnostics in developing countries. On the other hand, mechanical^{13–15} methods could lyse cells handily without specialized equipment and minimize protein denaturation resulting from the chemical reagent, electrical wave, or thermal shock during nonmechanical lysis processes. Consequentially, new mechanical cell-lysis chips based on LOC are recently being developed to satisfy the increasing market demand for a faster, cheaper, more facile and reliable process.

In general, the poor efficiency of cell lysis step limits the postanalysis, which is mostly affected by the concentration and the integrity of extracted proteins. Clearly, special designs for mechanical cell lysis are required to lyse cells rapidly and productively for a high concentration, the minimum loss of extracted proteins and direct analysis. Various types of LOC-based mechanical cell-lysis devices using nanoscale barbs,¹³ nanoblades¹⁴ or nanowires¹⁵ have extensively been investigated

during the past decade. However, they have focused on the integration of sharp structures within a microfluidic channel. Such devices might require a relatively long time to gather the desired protein concentration needed for analysis due to the slow flow rate of infusing cells, caused by increasing fluidic resistance in a limited number of microchannels. Most of them also have involved complicated fabrication processes in which many steps—such as lithography, alignment, reactive-ion etching, polymerization or bottom-up synthesis of nanostructures—were needed to make a whole device. Therefore, the development of a mechanical cell-lysis tool with a simple, robust, compact, faster, massive, and more reliable operation still remains as a practical engineering challenge.

In this paper, we propose a hierarchical silicon nanospikes membrane (HSSM) for facile, rapid, cost-effective, and high-throughput mechanical cell lysis without the assistance of additional reagents or power sources. The efficiency of cell lysis can be dramatically improved by the numerous self-decorated nanospikes on the periphery of the vertically aligned microchannels, which are tailored through maskless and single-step photoelectrochemical (PEC) etching. The direct assembly of the proposed membrane with a commercial syringe filter holder without changing any parts of the commercial products is also

Received: February 27, 2014

Accepted: May 7, 2014

Published: May 7, 2014

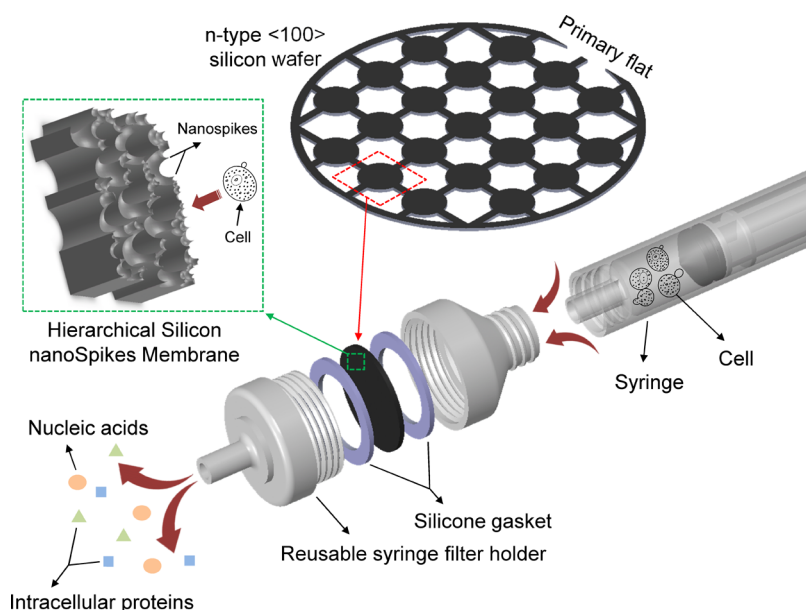


Figure 1. Schematic illustration of the direct assembly using the hierarchical silicon nanospikes membrane and a commercial hand-held syringe filter holder for mechanical cell lysis.

expected to minimize the fabrication cost as well as the preparation time for cell lysis.

Figure 1 depicts a schematic illustration of the overall cell-lysis device, composed of three main parts: a syringe filter holder, the proposed membrane and a commercial syringe. The HSSM is located in the middle of a syringe filter holder and fixed between two silicone gaskets to minimize the unwanted flow leakage along the edges of the membrane. This assembly makes cells pass directly across the HSSM, and thus, be ruptured by the ultrasharp nanospikes. The HSSM can be mass-fabricated in a silicon wafer scale and then diced properly for a desired design, as seen in Figure 1. The dimensions of diced HSSM from a wafer-scale membrane are based on specifications of a syringe filter holder. In this work, the membrane with a thickness of 120 μm and a diameter of 13 mm, which fits neatly into a commercial 13 mm syringe filter holder (Swinnex 13 Filter Holders, Millipore, MA), was tailored and used for experiments. The nanospikes surface of the HSSM faces the syringe tip. Therefore, cells inside the syringe connected to the filter holder with the HSSM can be rapidly ruptured with high throughput by simply pushing a plunger piston, as illustrated in Figure 1.

The overall fabrication process includes one single main process: PEC etching for forming a coherent microporous silicon membrane and decorating nanospikes in situ at the edges of fabricated microchannels by overetching. The detail fabrication process of the HSSM is included and illustrated with Figure S1 in the Supporting Information. The PEC etching in hydrofluoric (HF) acid solution, which is a highly anisotropic wet etching process, has traditionally been used for fabrication of microstructures in silicon substrates with aspect ratios over 10:1 and often 100:1.^{16–18} The formation mechanism of microporous silicon by PEC etching is a charge exchange between the semiconductor surface and fluoride ions in HF acid.¹⁹ Since the charge exchange mechanism is affected by the dopant type of the substrate,¹⁹ minority carriers in n-type semiconductors (i.e., holes) can be generated by photo-illumination, reducing the width of the carrier depleted space charge region (SCR).²⁰ Under anodic bias, these holes move to

the Si surface where Si–Si bonds weaken, allowing them to be etched by F^- ions in HF acid as seen in the circle showing the zoomed-in view of the Si surface in Figure S1a.¹⁹ Since anodic bias of n-type silicon always generates a SCR, the initiation of trenches occurs spontaneously at random positions and affects to the diameter of each trench by the local capturing efficiency for minority carriers.²¹ Unlike PEC etching with a mask pattern to generate uniform nucleation grooves by protecting the unexposed surface from F^- ions attack, a fully maskless PEC etching was intentionally used in this study to induce the sequent and discrete nucleation sites on the Si surface, which gradually etches on the periphery of the pre-etched trenches by initiating the formation of new trenches next to them (see Figure S1b, c in the Supporting Information). This continuative formation of trenches with a time lag remains as extremely narrow spaces between circular shapes of trenches because of geometry confinement, and thus, these unetched spaces become ultrasharp nanospikes, as seen in Figure S1d in the Supporting Information.

Images a and b in Figure 2 show the actual membrane size and a top surface view of the fabricated HSSM with an average pore diameter of 5.7 μm and an approximate porosity of 35.7% (14 000 pores/ mm^2) after PEC etching, respectively. The cross-section view shows high-aspect-ratio and straight microchannel arrays with an average length of 150 μm , as seen in Figure 2c. Figure 2d shows ultrasharp nanospikes on the periphery of the vertically aligned microchannels which will allow rapid cell disruptions immediately after infusing into the HSSM. Considering the flow rate of the cells-containing solution through the membrane, higher porosities are desirable for high-throughput lysis because the overall flow rate increases. However, because higher porosity can reduce the mechanical strength, and thus limit a finger force pushing a plunger piston, parametric investigations for various porosities will be needed for commercial adoption of the HSSM.²²

For the characterization of the cell-lysis performance by the HSSM, immortalized human keratinocyte cell-line (HaCaT, a gift from Berkeley Tissue Culture Facility), which is most often used in scientific research because of its highly preserved

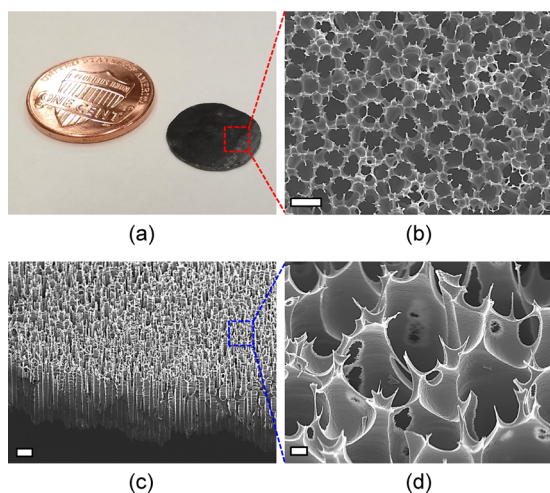


Figure 2. SEM images of photoelectrochemically etched hierarchical silicon nanopikes membrane: (a) size comparison of the fabricated 13 mm diameter membrane with a U.S. one-cent coin, (b) top surface view, (c) 45° tilted view, and (d) zoomed-in view of ultrasharp nanopikes. Scale bars: (b) 10, (c) 20, and (d) 1 μm .

differentiation capacity,²³ was used in this study. The detailed cell preparation for the experiment is described in the Supporting Information. After putting cells in a commercial syringe, the syringe filter holder assembled with the HSSM was directly connected to the syringe. Finally, the cells were injected toward the HSSM by simply pushing a plunger piston for the lysis. In order to obtain cell lysate by the acoustic and chemical methods, the sonication in a water bath (Branson 3510, Branson Ultrasonics, CT) at room temperature for 20 min and mixing suspended cells with a reagent (M-PER, Mammalian Protein Extraction Reagent, Thermo Scientific, MA) followed by incubation at room temperature for 10 min, was conducted for a comparative analysis, respectively.

Figure 3a shows an experimental image of the mechanical cell-lysis process using the fabricated membrane assembled with a commercial syringe filter holder and directly connected to a

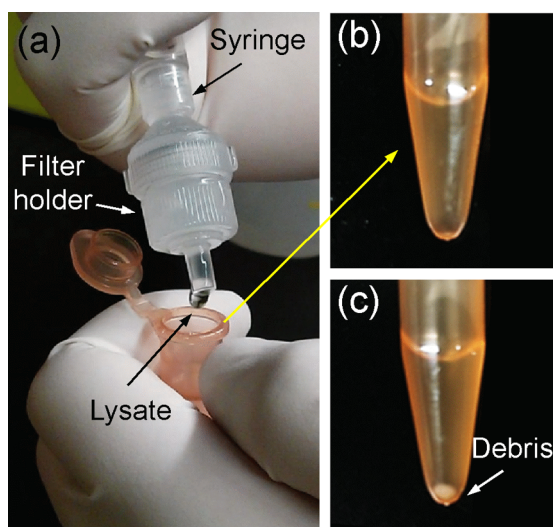


Figure 3. Experimental image of (a) the developed mechanical cell-lysis process and (b) the lysate without membrane debris after centrifugation compared to the (c) deposited membrane debris in the lysate obtained by conventional chemical lysis.

syringe. After lysis, the lysate of the HaCaT cells was directly dropped into a microcentrifuge tube, as seen in Figure 3a, and centrifuged at 14 000 rpm for 15 min. Figure 3b shows that the lysate after the developed mechanical cell lysis does not contain any cell membrane debris, whereas the routine centrifugation was necessary for the lysate obtained by conventional chemical cell lysis to deposit the debris (Figure 3c). Therefore, the HSSM acts both as a cell disrupter and a filter after disruption, which allows rapid cell lysis and direct analysis by significantly reducing the postprocess and maintaining the integrity of purified samples, respectively. The scanning electron microscope (SEM) image of the HSSM before and after cell lysis is shown in images a and b in Figure 4, respectively. The HaCaT cells with an average diameter of 20 μm were ruptured by ultrasharp silicon nanopikes, whereas the structural shape of the nanopikes remains as before lysis without breakages, which might be caused by the force of inertia resulting from the flow rate across the HSSM. Figure 4c shows the zoomed-out view of the ruptured and filtrated debris of HaCaT cell membrane. In order to confirm that cells were not able to pass through the HSSM without lysing, the optical image of HaCaT cells before and after the HSSM cell lysis was observed using a bright field microscope as shown in Figure S2a, b in the Supporting Information, respectively. These results demonstrate that HaCaT cells were successfully destructed and filtrated after lysing (i.e., passing through the HSSM) while the cells were visually observed before lysing. As the HSSM filters cell membrane debris out by anchoring them between nanopikes, it allows rapid cell lysis and direct analysis due to the reduced postprocess step. For further secure filtration, a commercial membrane filter (Omnipore, 0.2 μm , Milipore, MA) can be additionally placed behind the HSSM.

To quantitatively evaluate the lysis efficiency of the HSSM, we performed nonspikes silicon membrane lysis, conventional acoustic lysis, and chemical lysis and compared it to the one prepared using the developed mechanical cell-lysis method. For the nonspikes silicon membrane, the PEC etching was carried out again with a reduced anodization time to prevent the formation of nanopikes by overetching (i.e., the etching was stopped at the Figure S1c step). Figure S3 in the Supporting Information shows the SEM images of the nonspikes silicon membrane, which was etched for 100 min. For quantitative analysis, concentrations of intracellular proteins and nucleic acids were measured for all methods using a spectrophotometer (NanoDrop 2000, Thermo Scientific, MA). The wavelengths to measure the optical absorbance of intracellular proteins and nucleic acids in soluble cell lysates were 280 and 260 nm, respectively.

The total protein and nucleic acid concentrations in each lysate are shown in Figure 5 with p-values. As shown in the figure, it was found that both the intracellular protein ($1018 \pm 60.1 \text{ mg mL}^{-1}$) and the nucleic acid concentrations ($99.3 \pm 19.1 \text{ ng } \mu\text{L}^{-1}$) via the developed mechanical cell lysis using the HSSM were higher than those obtained by the conventional acoustic ($204 \pm 40.36 \text{ mg mL}^{-1}$ and $25.5 \pm 5.99 \text{ ng } \mu\text{L}^{-1}$) and chemical ($898.67 \pm 22.03 \text{ mg mL}^{-1}$ and $89.55 \pm 2.41 \text{ ng } \mu\text{L}^{-1}$) methods even though the total lysis time required for the developed method was less than 1 min. Figure S4 in the Supporting Information shows the intracellular protein species separated by gel electrophoresis verifying that the HaCaT cell lysing by the developed mechanical method was able to extract various proteins from the cell. The results demonstrate that the HSSM mechanical cell lysis is superior to the conventional

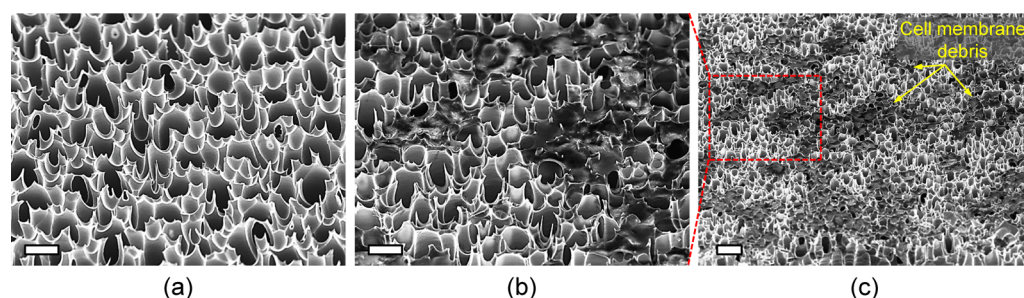


Figure 4. SEM images of (a) hierarchical silicon nanopikes membrane before cell lysis, (b) ruptured HaCaT cell membranes by ultrasharp nanopikes after cell lysis and (c) zoomed-out view of ruptured and filtrated debris of HaCaT cell membrane. Scale bars: (a) 10, (b) 10, and (c) 20 μm .

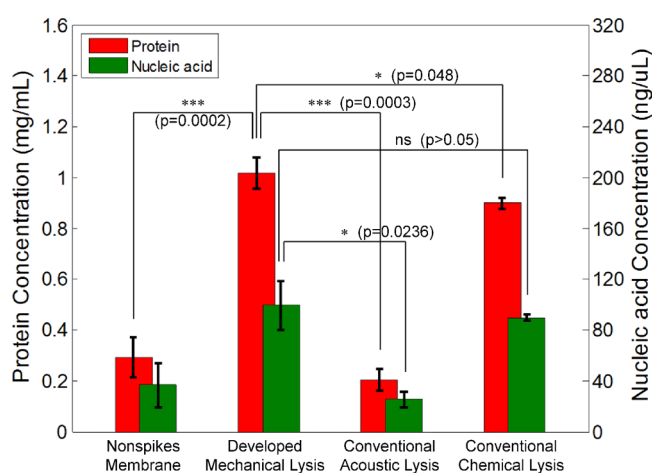


Figure 5. Comparison of protein and nucleic acid concentrations after HaCaT cell lysing between the developed mechanical cell lysis method and the conventional methods.

acoustic method and comparable to the chemical method. To investigate the significance of nanopikes, cell lysis with a nonspikes silicon membrane, which might rupture cells by the fluidic shear force between the cell membrane and microchannel wall, was also conducted in the same manner resulting in the protein ($292 \pm 79.5 \text{ mg mL}^{-1}$) and nucleic acid concentrations ($36.5 \pm 17.01 \text{ ng } \mu\text{L}^{-1}$), which were approximately three times lower than those obtained by the HSSM cell lysis.

To demonstrate the reliability of cell lysis by the fabricated HSSM, hepatocellular carcinoma cell-line (HepG2, a gift from Berkeley Tissue Culture Facility), which has much smaller diameter (10 μm) than HaCaT cell, was analyzed in the same manner as the HaCaT cell lysing. As a result, the total protein and nucleic acid concentrations after HepG2 cell lysing were shown in Figure S5 in the Supporting Information showing quantitatively higher values than those obtained by conventional methods. Therefore, the developed mechanical cell lysis with a tailored silicon nanopikes membrane, which also can be mass-fabricated for commercialization, is a much more convenient, rapid, and efficient method than the conventional acoustic, mechanical, and chemical approaches.

In this letter, a hierarchical silicon nanopikes membrane was developed for rapid and high-throughput mechanical cell lysis to extract intracellular proteins and nucleic acids without the assistance of chemicals, external power sources or microfluidic platforms. A demonstration of this membrane was shown with a tailored fabrication process by the PEC overetching, intention-

ally inducing sequent and discrete nucleation sites on the Si surface. The ultrasharp nanopikes were successfully fabricated along the edges of vertically aligned microchannel arrays to rupture cell membranes as well as to filter out membrane debris. For the mechanical cell lysis, the fabricated membrane was directly assembled with a commercial syringe filter holder and then connected to a syringe. The HaCaT and HepG2 cell lysates prepared by the HSSM mechanical cell lysis method had quantitatively higher intracellular protein and nucleic acid concentrations than those obtained by conventional acoustic and chemical lysis methods. The hand-held HSSM mechanical cell lysis method allowed successful, efficient and high-throughput cell lysis within a short period of time compared to conventional methods which require complicated multiple steps and expensive equipment such as a sonicator and centrifuge. This study is a first step toward demonstrating the feasibility of a cost-effective and simple cell lysis to address the sample preparation requirements for point-of-care diagnostics of a disease in developing countries by reducing postprocess time and the use of expensive equipment.

■ ASSOCIATED CONTENT

Supporting Information

Schematic illustration of the fabrication process, SEM images of the HSSM with different anodization times, optical microscope image for populations of the HaCaT cells before and after lysis, description of cell preparation, protein species of HaCaT cells separated by gel electrophoresis, and protein/nucleic acid concentrations after HepG2 cell lysing. This material is available free of charge via the Internet at <http://pubs.acs.org/>.

■ AUTHOR INFORMATION

Corresponding Author

*E-mail: hyso@berkeley.edu.

Notes

The authors declare no competing financial interest.

■ ACKNOWLEDGMENTS

This work was supported by the grants from the National Heart Lung and Blood Institute of the NIH as a Program of Excellence in the Nanotechnology award (HHSN268201000043C), RO1HL096796-02, and RO1AI088023-03. This work also supported by the Pioneer Research Center Program (NRF-2012-0009575) from the National Research Foundation of Korea.

■ REFERENCES

- (1) Fu, A. Y.; Spence, C.; Scherer, A.; Arnold, F. H.; Quake, S. R. A Microfabricated Fluorescence-Activated Cell Sorter. *Nat. Biotechnol.* **1999**, *17*, 1109–1111.
- (2) Legendre, L. A.; Bienvenue, J. M.; Roper, M. G.; Ferrance, J. P.; Landers, J. P. A Simple, Valveless Microfluidic Sample Preparation Device for Extraction and Amplification of DNA from Nanoliter-Volume Samples. *Anal. Chem.* **2006**, *78*, 1444–1451.
- (3) Nevill, J. T.; Cooper, R.; Dueck, M.; Breslauer, D. N.; Lee, L. P. Integrated Microfluidic Cell Culture and Lysis on a Chip. *Lab Chip* **2007**, *7*, 1689–1695.
- (4) Irimia, D.; Tompkins, R. G.; Toner, M. Single-Cell Chemical Lysis in Picoliter-Scale Closed Volumes Using a Microfabricated Device. *Anal. Chem.* **2004**, *76*, 6137–6143.
- (5) Han, F.; Wang, Y.; Sims, C. E.; Bachman, M.; Chang, R.; Li, G. P.; Allbritton, N. L. Fast Electrical Lysis of Cells for Capillary Electrophoresis. *Anal. Chem.* **2003**, *75*, 3688–3696.
- (6) Wang, H.-Y.; Bhunia, A. K.; Lu, C. A Microfluidic Flow-through Device for High Throughput Electrical Lysis of Bacterial Cells Based on Continuous dc Voltage. *Biosens. Bioelectron.* **2006**, *22*, 582–588.
- (7) Bao, N.; Lu, C. A Microfluidic Device for Physical Trapping and Electrical Lysis of Bacterial Cells. *Appl. Phys. Lett.* **2008**, *92*, 214103.
- (8) Holmes, D. S.; Quigley, M. A Rapid Boiling Method for the Preparation. *Anal. Biochem.* **1981**, *197*, 193–197.
- (9) Rau, K. R.; Guerra, A.; Vogel, A.; Venugopalan, V. Investigation of Laser-Induced Cell Lysis Using Time-Resolved Imaging. *Appl. Phys. Lett.* **2004**, *84*, 2940–2942.
- (10) Hellman, A. N.; Rau, K. R.; Yoon, H. H.; Venugopalan, V. Biophysical Response to Pulsed Laser Microbeam-Induced Cell Lysis and Molecular Delivery. *J. Biophotonics* **2008**, *1*, 24–35.
- (11) Kaufman, G. E.; Miller, M. W.; Griffiths, T. D.; Ciaravino, V.; Carstensen, E. L. Lysis and Viability of Cultured Mammalian Cells Exposed to 1 MHz Ultrasound. *Ultrasound Med. Biol.* **1977**, *3*, 21–25.
- (12) Ward, M.; Wu, J.; Chiu, J. F. Ultrasound-Induced Cell Lysis and Sonoporation Enhanced by Contrast Agents. *J. Acoust. Soc. Am.* **1999**, *105*, 2951–2957.
- (13) Di Carlo, D.; Jeong, K.-H.; Lee, L. P. Reagentless Mechanical Cell Lysis by Nanoscale Barbs in Microchannels for Sample Preparation. *Lab Chip* **2003**, *3*, 287–291.
- (14) Yun, S.-S.; Yoon, S. Y.; Song, M.-K.; Im, S.-H.; Kim, S.; Lee, J.-H.; Yang, S. Handheld Mechanical Cell Lysis Chip with Ultra-Sharp Silicon Nano-Blade Arrays for Rapid Intracellular Protein Extraction. *Lab Chip* **2010**, *10*, 1442–1446.
- (15) Kim, J.; Hong, J. W.; Kim, D. P.; Shin, J. H.; Park, I. Nanowire-Integrated Microfluidic Devices for Facile and Reagent-Free Mechanical Cell Lysis. *Lab Chip* **2012**, *12*, 2914–2921.
- (16) Lehmann, V. The Physics of Macropore Formation in Low Doped n-Type Silicon. *J. Electrochem. Soc.* **1993**, *140*, 2836–2843.
- (17) Föll, H.; Christophersen, M.; Carstensen, J.; Hasse, G. Formation and Application of Porous Silicon. *Mater. Sci. Eng., R* **2002**, *39*, 93–141.
- (18) Sun, G.; Zhao, X.; Kim, C.-J. Fabrication of Very-High-Aspect-Ratio Microstructures in Complex Patterns by Photoelectrochemical Etching. *J. Microelectromech. Syst.* **2012**, *21*, 1504–1512.
- (19) Bell, T. E.; Gennissen, P. T. J.; DeMunter, D.; Kuhl, M. Porous Silicon as a Sacrificial Material. *J. Micromech. Microeng.* **1996**, *6*, 361–369.
- (20) Bail, M.; Schulz, M.; Brendel, R. Space-Charge Region-Dominated Steady-State Photoconductance in Low-Lifetime Si Wafers. *Appl. Phys. Lett.* **2003**, *82*, 757–759.
- (21) Lehmann, V.; Föll, H. Formation Mechanism and Properties of Electrochemically Etched Trenches in n-Type Silicon. *J. Electrochem. Soc.* **1990**, *137*, 653–659.
- (22) So, H.; Cheng, J. C.; Pisano, A. P. Nanowire-Integrated Microporous Silicon Membrane for Continuous Fluid Transport in Micro Cooling Device. *Appl. Phys. Lett.* **2013**, *103*, 163102.
- (23) Schoop, V. M.; Mirancea, N.; Fusenig, N. E. Epidermal Organization and Differentiation of HaCaT Keratinocytes in Organotypic Coculture with Human Dermal Fibroblasts. *J. Invest. Dermatol.* **1999**, *112*, 343–353.